Extended Abstracts of the 2006 International Conference on Solid State Devices and Materials, Yokohama, 2006, pp. 288-289

C-5-2

# Low Power Operation of Non-volatile Hafnium Oxide Resistive Memory

Heng-Yuan Lee[1], Pang-Shiu Chen[2], Ching-Chiun Wang[1], Siddheswar Maikap[1],
Pei-Jer Tzeng[1], Cha-Hsin Lin[1], Lurng-Shehng Lee[1], and Ming-Jinn Tsai[1]

[1]Electronics and Optoelectronics Research Laboratory, Industrial Technology Research Institute
Chutung, Hsinchu 310, Taiwan
[2]Department of Materials Science and Engineering, MingShin University of Science & Technology
Hsinfong, Hsinchu 304, Taiwan
Phone : 886-3-5913859, Fax : 886-3-5917690, E-mail : hengyuan@itri.org.tw

## Introduction

Owing to the bi-stable resistance switching property and being compatible with the semiconductor manufacturing process, binary oxides, such as NiO [1], $TiO_2$ [2], $Al_2O_3$, have attracted much attention in recent years. Several methods have been proposed to prepare the transition metal oxide including oxidation of metal, metal sputtering in oxygen ambient, or MOCVD. However, these devices have high operation current (> 1mA) which may limit their application on the circuit [1]. Atomic layer deposition (ALD) can fabricate well-controlled quality of transition metal oxides without radiation damage. In this study, a commercial ALD system is used to deposit the non-stoichiometric Hafnium oxide layers. As the result, a resistive memory device consisting of $HfO_{2-x}$ and with low operation current (~ 100μA) is realized.

## Device Fabrication

Resistive memory in this work is fabricated as following: TiN film is covered on the 8 " wafer as bottom electrode (BE). A nominal 20-nm-thick $HfO_{2-x}$ is deposited on the prior substrate by ALD system (ASM, polygon 8200) at 300 °C. Hafnium tetrachloride ($HfCl_4$) and water ($H_2O$) are used as reactants. The surface morphology of $HfO_{2-x}$/TiN/Si samples is examined by atomic force microscopy (AFM) in tapping mode. Top electrode Pt is then deposited by sputtering method with a shadow mask at room temperature. Microstructure of Pt/$HfO_{2-x}$/TiN/Si is characterized by the cross-sectional transmission electron microscopy (XTEM). X-ray photon spectroscopy (XPS) is used to check the composition of $HfO_{2-x}$. Finally, C-V and I-V characteristics of the memory device are measured by HP4284 LCR meter and HP4156 semiconductor parameter analyzer, respectively. From the result of C-V measurement, the dielectric constant of as-grown $HfO_{2-x}$ film is ~21 and the current density of the device is ~ $1\times10^{-8}$ A/cm$^2$ at 1V.

## Results and Discussion

Fig. 1 shows the high resolution XTEM of Pt/$HfO_{2-x}$/TiN/Si. From the diffraction pattern and lattice image analysis, it indicates that crystal structure of $HfO_{2-x}$ layer is monoclinic phase. The poly-grain characteristic of $HfO_{2-x}$ thin film on TiN/Si results in rough surface morphology. Fig. 2 is the AFM image of $HfO_{2-x}$/TiN/Si with root-mean-square surface roughness of ~ 8.7 Å. In Fig. 3, the composition depth profile of $HfO_{2-x}$ on TiN is presented. It is found that $HfO_{2-x}$ layer shows no residual Cl (below detection limit of 0.5%) and the atomic ratio of Hf and O is ~ 1.5, which suggests that metal excess non-stoichiometric $HfO_{2-x}$ film is formed by ALD method.

This metal-insulator-metal (MIM) capacitor device exhibits bi-stable resistance switching property after soft breakdown-like formation process at 5.4 V and current compliance of 100 uA. Followed by formation process, measurement of DC switching is performed successfully. Fig. 4 shows some typical bi-stable switching I-V curves. During measurement, the SET process (from $R_{HIG}$ to $R_{LOW}$) is clamped at 100 μA, and maximum operation current, which corresponds to the RESET process (from $R_{LOW}$ to $R_{HIGH}$), is also around 100 μA. Fig. 5 is the evolution of $R_{HIGH}$ and $R_{LOW}$ at 0.5 V during 300 cycles of switching. The distribution of $R_{HIGH}$ and $R_{LOW}$ values are presented in Fig. 6. Fluctuation of $R_{HIGH}$ values may be due to non-uniform disruption of filament in the $HfO_{2-x}$ films. During the switching cycles, most of R ratios ($R_{HIGH}/R_{LOW}$) with the mean values of 180 are larger than 10, as shown in the inset of Fig. 6. Fig. 7 shows the operation voltage distribution. Most of SET and RESET voltages are around 2.3 V and 1.6 V, respectively. The electrical results indicate that Pt/$HfO_{2-x}$/TiN capacitor is suitable for a low power operation resistive switching device.

For nonvolatile memory application, retention testing of this MIM device is carried out at 85 °C for 6 hrs. The results of retention testing, as shown in Fig. 8, give promise of 10 years lifetime. Also, IV characteristics of the device at 20 °C and 85 °C are compared and shown in Fig. 9. Though leakage of $R_{LOW}$ state obeys ohmic transport, filament theory is not enough to explain the less temperature-dependent leakage of this device [3]. To explore the scalability, the dependence of cell size on $R_{LOW}$ and $R_{FRESH}$ are depicted in Fig. 10. $R_{LOW}$ has less size dependence but the resistivity of as-grown $HfO_{2-x}$ ($R_{FRESH}$) is inversely proportional to the size. Less size dependence of $R_{LOW}$ may be due to localized filament [4], and provides great advantages in scaling down of MIM capacitor. Fig. 11 shows the electrode-dependence of the switching property of this MIM device. High power and unstable switching property of this MIM capacitor are found in negative bias operation. Electrode dependence may be due to oxidation-intended BE TiN [4].

## Conclusions

Using ALD system to fabricate metal excess HfO film as the resistive switching layer, a low power operation resistive memory with 100uA RESET current has been proven feasible.

## References

[1]I.G. Baek et al., IEDM Tech. Dig., p587-590, 2004

[2]Christina Rohde et al., Appl. Phys. Lett, **86**, 262907, 2005

[3]K. Kinoshita et al., Nonvolatile Semiconductor Memory Workshop, p84-85, 2006

[4]B.J. Choi et al., J. Appl. Phys., **98**, 033715, 2005


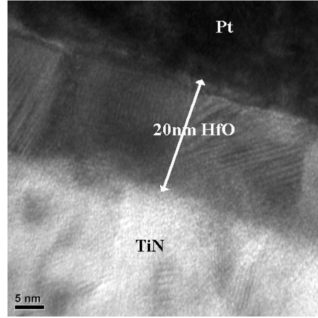


Fig. 1 High resolution XTEM image of Pt/HfO/TiN capacitor on Si

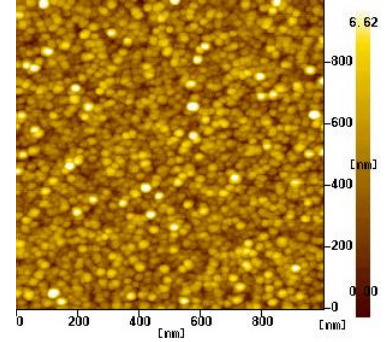

Fig. 2 AFM image of HfO/TiN on Si

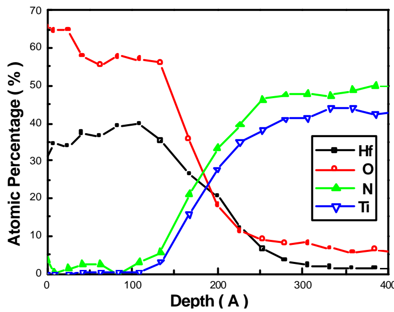


Fig. 3 XPS composition depth profile of HfO/TiN on Si

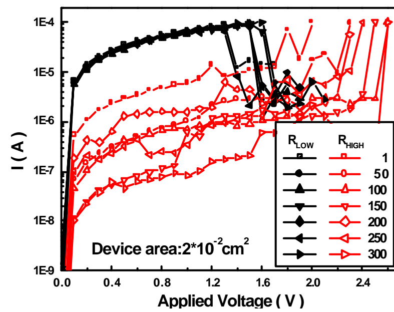


Fig. 4 Typical bi-stable switching I-V curves of Pt/HfO/TiN capacitor

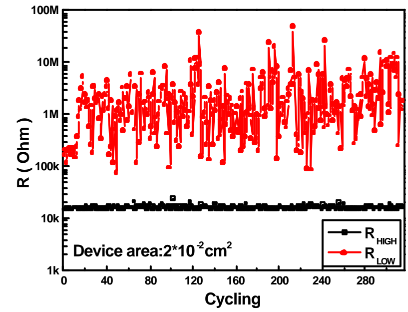


Fig. 5 Evolution of $R_{HIGH}$ and $R_{LOW}$ (at 0.5 V) of Pt/HfO/TiN capacitor

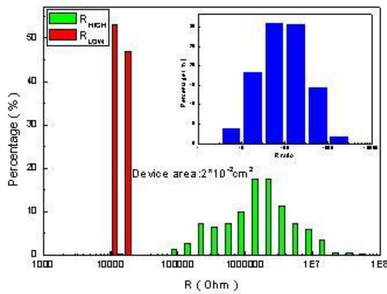

Fig. 6 Distribution of $R_{HIGH}$ and $R_{LOW}$ of Pt/HfO/TiN capacitor

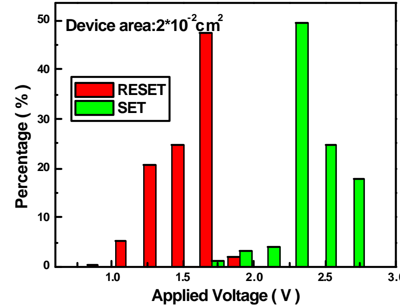


Fig. 7 Distribution of operation voltages of Pt/HfO/TiN capacitor

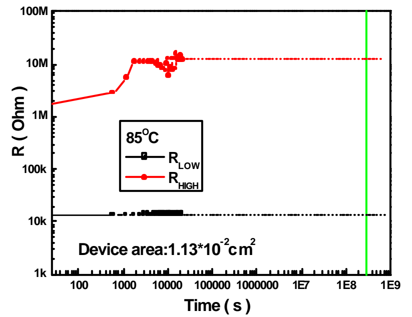


Fig. 8 Retention of Pt/HfO/TiN capacitor at 85 °C

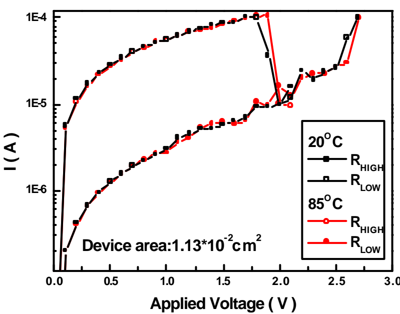


Fig. 9 Comparison of switching property of Pt/HfO/TiN capacitor at 20 °C and 85 °C

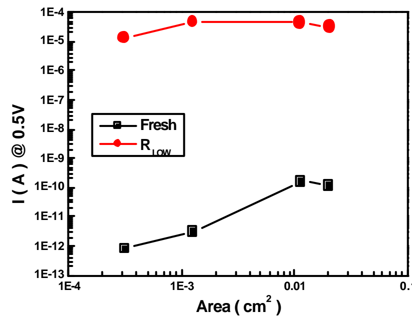


Fig. 10 Cell size dependence of $R_{FRESH}$ and $R_{LOW}$ of Pt/HfO/TiN capacitor

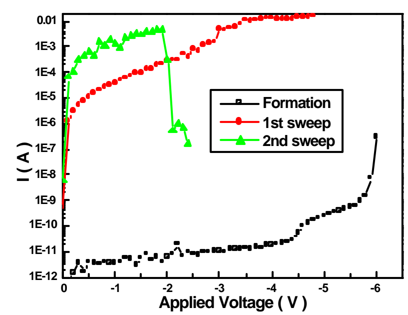


Fig. 11 Unstable switching properties of Pt/HfO/TiN capacitor under negative bias operation